Combining discrepancy analysis with sensorless signal resampling for condition monitoring of rotating machines under fluctuating operations

T Heyns, P S Heyns and R Zimroz

This paper proposes a novel framework for monitoring the condition of a rotating machine (for example a gearbox or a bearing) that may be subject to load and speed fluctuations. The methodology is especially relevant in situations where no (or only noisy) shaft angular position measurements are available. Shaft angular position reference measurements are often not available due to physical constraints that render it difficult to install tachometers or encoders on the shaft of interest. The proposed methodology aims to simplify the task of monitoring a time-varying vibration signal by using a neural network to filter out the normal vibration components that generally tend to dominate the signal. The neural network may be optimised without the need for extensive datasets that are representative of different machine fault conditions. The envelope of the filtered signal is referred to as a discrepancy transform, since the discrepancy signal indicates the presence of fault-induced signal distortions. The discrepancy signal tends to be significantly simpler (smoother) than the original vibration waveform and may thus be resampled using a less accurate reference signal than would be required to resample the original waveform. A numerical gear model is used to illustrate the diagnostic potential of the proposed methodology.

1. Introduction

The performance of many conventional machine condition monitoring strategies (for example spectral analysis) tends to be impeded if the machine is subject to fluctuating operating conditions[1]. Fluctuating operating conditions tend to induce amplitude, frequency and phase modulation in the vibration signals, hence destroying the wide-sense stationarity of the signal, which is implicitly assumed when applying Fourier analysis[2].

T Heyns is with the Council for Scientific and Industrial Research South Africa, MSM, SST, Pretoria, South Africa, 0081. Tel: +27 7214 3879; Email: theoheyns@gmail.com

P S Heyns is with the Dynamic Systems Group, Department of Mechanical and Aeronautical Engineering, University of Pretoria, Pretoria, South Africa, 0081. Tel: +27 8244 76068; Email: stephan.heyns@up.ac.za

Radoslaw Zimroz is with the Diagnostics and Vibro-Acoustics Science Laboratory, Wroclaw University of Technology, Pl Teatralny 2, Wroclaw, 50-051, Poland. Tel: +48 71 320 6849; Email: radoslaw.zimroz@pwr.wroc.pl

Order tracking, where the time domain signal is resampled at fixed angular intervals, tends to suppress some of the frequency modulating effects induced by speed fluctuation[2]. Angular signal resampling requires a shaft angular position reference signal. Due to physical and financial constraints, it is not always possible to install the additional equipment (for example an optical encoder or tachometer) that is required to accurately measure the shaft angular position[3]. For this reason, research[3,4,5] has been conducted to determine how the shaft angular position may be directly estimated from the vibration signal. Bonnardot *et al*[3] consider a phase demodulation technique, where a shaft harmonic is selected and isolated by means of appropriate filtering. The Hilbert transform of the signal is used to represent the signal in its analytic form. This subsequently allows for the extraction of the phase angle of the identified frequency component. Urbanek *et al*[4] investigate the relative performance of the phase-based methodology first proposed by Bonnardot *et al*[3] with an amplitude-based method. In addition, they also briefly refer to a methodology that allows for estimating the relative shaft speed by inspecting the local maxima in a spectrogram of the vibration signal. The proposed methodology avoids the need for expensive additional transducers to measure the shaft angular position, but is somewhat limited both in terms of the accuracy and the range of speeds to which it may be applied[3,4]. Combet and Gelman[5] extend the algorithm proposed by Bonnardot *et al*[3] by allowing for a method whereby the mesh harmonic, which will be narrow-band demodulated and used to estimate the shaft phase, may automatically be selected based on the local signal-to-noise ratio. Further research on sensorless frequency/speed estimation via timescale and time-frequency analysis can also be found in works by Combet and Zimroz[6], Millioz and Martin[7], as well as Zimroz *et al*[8,9]. Interesting results have also been obtained by the research team led by Antoniadis, by means of parametric modelling and by implementing the Teager-Kaiser operator[10,11].

Residual signal analysis refers to a collection of techniques that aim to remove the regular components from a vibration signal, so that only fault-induced signal components remain. A number of different approaches for obtaining residual signals have been investigated in literature. Stewart[12] computes a residual signal by removing the gear meshing harmonics and its adjacent sidebands from the signal average spectrum before converting the signal back to the angle domain. Wang and Wong[13] use an autoregressive (AR) filter to model the vibration waveform, which is recorded when the gearbox is still in a good condition. A novel signal may be subsequently transformed to a residual signal by computing

the difference between the measured signal and the one-step-ahead AR predictions. Heyns *et al*[14] extend Wang and Wong's idea to better deal with time-varying operating conditions by implementing multiple parallel AR models. The different AR models represent the machine behaviour for different operating conditions. Apart from the abovementioned techniques, it should be recalled that Antoni and Randall used so-called self-adaptive noise cancellation (SANC) techniques based on a least mean squares (LMS) adaptive filter[15]. Zirmoz and Bartelmus have applied normalised LMS in order to extract a residual signal from a vibration signal measured on a belt conveyor pulley drive unit in the presence of time-varying speed/load conditions[16]. An advanced approach that uses an adaptive Schur filter was recently proposed by Makowski and Zimroz[17].

This paper proposes a novel framework for monitoring the condition of a rotating machine (for example a gearbox or a bearing) that may be subject to load and speed fluctuations. The methodology is based on the combined use of envelope residual signal analysis along with approximate signal resampling. This allows for vibration-based condition monitoring under time-varying operating conditions, even when no accurate shaft angular position measurements are available. A feed-forward neural network is used to filter the time-varying vibration signal in order to remove the signal components that correspond to a healthy vibration signal. The envelope of the residual signal is then computed by means of the Hilbert transform. The obtained transform is referred to as a discrepancy transform, since the discrepancy signal indicates the presence of fault-induced signal distortions (discrepancies) that are not present in the baseline (healthy) signal. The discrepancy signal tends to be significantly simpler and smoother than the original vibration waveform. The instantaneous shaft angular speed may then be estimated from the original vibration signal and used to approximately resample the discrepancy signal. The resampling stage accounts for significant (but slowly varying) frequency modulation, while the smooth character of the discrepancy signal renders the transform more robust to noise in the estimated shaft angular reference signal.

This paper uses a numerical gear model to briefly illustrate how the combined use of discrepancy analysis and approximate signal resampling may be used to monitor the condition of a rotating machine that is subject to time-varying operations, even when no angular position sensor is available.

2. Methodology

The methodology implemented in this paper is summarised in Figure 1.

The first step is concerned with computing a residual signal by means of comparing a novel vibration signal to the reference neural network (NN) model. The reference model represents the vibration response from the gearbox while it is in a good condition. It is assumed that the baseline vibration response is representative of the different possible operating conditions. These conditions are represented by multiple snippets of time series, which are appended to the training data. A single non-linear NN regression model is used to represent the complete training dataset. The performance of the NN is compared to

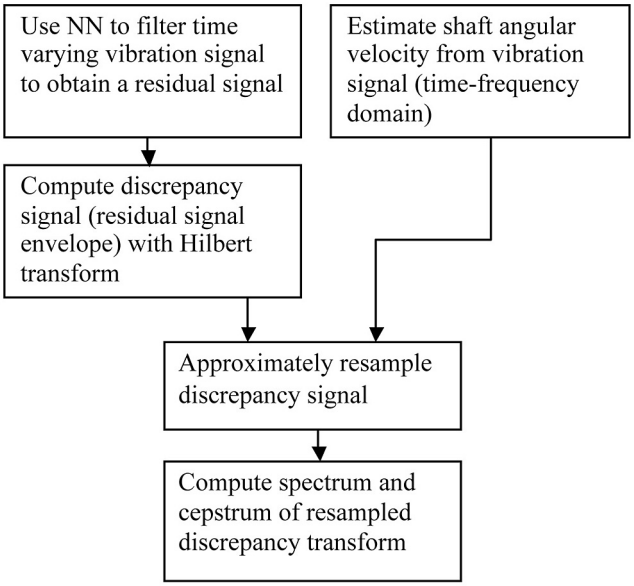

Figure 1. Flowchart of the proposed methodology

that of a linear AR model. Once the residual signal is available, its analytic representation is obtained by means of the Hilbert transform. The analytic representation is used to compute the signal envelope, which is also referred to as a discrepancy signal. The discrepancy signal indicates the time instances and the extent to which the measured signal deviates from the baseline model.

The information contained in the discrepancy transform is much simpler (lower bandwidth) compared to the original vibration waveform and is hence less sensitive to noise in the reference signal that will be used for resampling. The relative shaft rotational velocity may be estimated from the vibration waveform. In this paper, a simple clustering approach that considers the local maxima in the spectrogram is used to estimate the relative shaft speed. Depending on the application, more advanced signal resampling methodologies may be desirable, however, the aim of this paper is to illustrate that the methodology may be implemented even with only approximate relative speed measurements. Lastly, the spectrum and cepstrum of the discrepancy transform are computed and interpreted.

2.1 *Time-series modelling*

The residual signal r_t at time instant t is computed as the difference between the observed signal value x_t at time instant t and the one-step-ahead model prediction $\hat{x}_t$, so that $r_t = x_t - \hat{x}_t$.

2.2.1 *Autoregressive (AR) model*

An AR model of order p is described by $\hat{x}_t = \sum_{k=1}^{p} a_k x_{t-k}$, so that the expected value $\hat{x}_t$ differs from the real waveform x_t by some white noise $b_0\sigma_t$. The AR spectral model, which is an all-pole model, may be shown to be good for modelling spectra with sharply-defined peaks[18]. The AR coefficients are optimised based on a least squares error criterion.

2.2.2 *Neural network regression*

A simple feed-forward neural network (NN) is also used to represent the time-series data. Similar to the AR model, the NN is

implemented so as to estimate the one-step-ahead prediction $\hat{x}_t$ based on the p most recent signal observations $\{x_{t-k}\}_{k=1}^{p}$. A NN architecture with sigmoid activation functions in the hidden layer and a linear activation function in the output layer is selected. To account for a possible constant offset, a bias value of one is added to the inputs. It has been shown that when this architecture is employed with a sufficient number of nodes in the hidden layer, it is a universal approximator that is capable of representing any continuous function to arbitrary precision[19].

The training dataset consists of n input vectors, which correspond to the n target values (which are the one-step-ahead predictions). The neural network may be summarised by Equation (1), where $g(\circ)$ represents the sigmoid activation function:

$$\hat{x}_t = \left(\sum_{j=1}^{p} w_j g\left(\sum_{k=1}^{n} w_{jk} x_{t-k} + w_j\right) + w_b\right) \quad \text{..... (1)}$$

The network is trained in Matlab by using backpropagation (efficient gradient descent) optimisation, whereby the weights of the networks are adjusted so as to minimise the sum squared error (SSE) between the predicted values $\hat{x}_t$ of the network and the target values. The optimisation procedure is terminated (convergence assumed) when the neural network's performance on an independent validation dataset reaches a minimum.

2.3 Hilbert transform envelope

To compute the residual envelope, the residual signal must first be represented in its analytic form z. The analytic form comprises the real component r (the original residual signal) and the imaginary component $jH(r)$:

$$z = r + jH(r) \quad \text{..... (2)}$$

The imaginary part is computed by means of the Hilbert transform:

$$H(r) = \frac{1}{\pi}\int_{-\infty}^{\infty} r(\tau)\frac{1}{t-\tau}d\tau \quad \text{..... (3)}$$

and the residual envelope (or discrepancy signal) d is subsequently computed as the complex modulus:

$$d = \sqrt{r^2 - \left(jH(r)^2\right)} \quad \text{..... (4)}$$

2.4 Sensorless relative speed estimation and resampling

The relative shaft speed is estimated directly from the vibration signal. As discussed in the introduction, there are different methodologies that may be followed to estimate the shaft angular position (or velocity) directly from the vibration signal. The speed estimation method employed in this paper is based on a time-frequency analysis. In essence, the local maxima of a spectrogram (magnitude of the short-time Fourier transform) are computed. Each local maximum point is associated with a unique time t^*, magnitude m^* and frequency f^* value.

Visual inspection is used to select a frequency component (the gear meshing frequency or one of its higher harmonics) that is synchronous with the frequency modulation. The selected frequency component needs to be free from other parasite (interfering) frequency components.

Beginning at a manually selected point, a clustering algorithm is employed that groups together local maxima based on a nearest neighbour criterion. The distance δ_{ij} between neighbouring points i and j (local maxima) is based on the modulus of the scaled time difference Δt_{ij}, magnitude difference Δm_{ij} and frequency difference Δf_{ij} between the two points:

$$\delta_{ij} = \sqrt{\left(\frac{\Delta t_{ij}}{a}\right)^2 + \left(\frac{\Delta m_{ij}}{b}\right)^2 + \left(\frac{\Delta f_{ij}}{c}\right)^2} \quad \text{..... (5)}$$

In this paper, the scaling factors a, b and c are selected so as to unit normalise the standard deviation for each of the clustering dimensions. It is expected that the scaling factors will require different criteria for different problems.

Once all the maxima that are related to the frequency component of interest have been clustered, they are low-pass filtered and used to resample the vibration signal.

3. Case study

3.1 Gear model

The proposed methodology is briefly investigated on a dataset, which is simulated based on the same gear model as implemented by Heyns *et al*[14]. This dynamic gear model is inherently very simple and comprises a set of second-order differential equations that relate the forcing function (applied torque), as well as the lumped mass, stiffness and friction coefficients, to the vibration response of the gear casing. The simple gear model is preliminarily used to investigate the efficiency of the proposed methodology. There are several assumptions that could be improved for gearbox dynamic-oriented modelling as provided in[20] or recently in[21,22]. Research conducted by Jia *et al*[23] indicates that it is appropriate to approximate the gear mesh stiffness as a square function. The magnitude of the meshing stiffness k_m is selected to fluctuate by approximately 20% around the mean value. It is common to model the effects of tooth faults, such as a tooth root crack, by reducing the stiffness of the affected tooth[23].

The stiffness coefficients k_1, k_2, k_3 and k_4 are assumed to satisfy

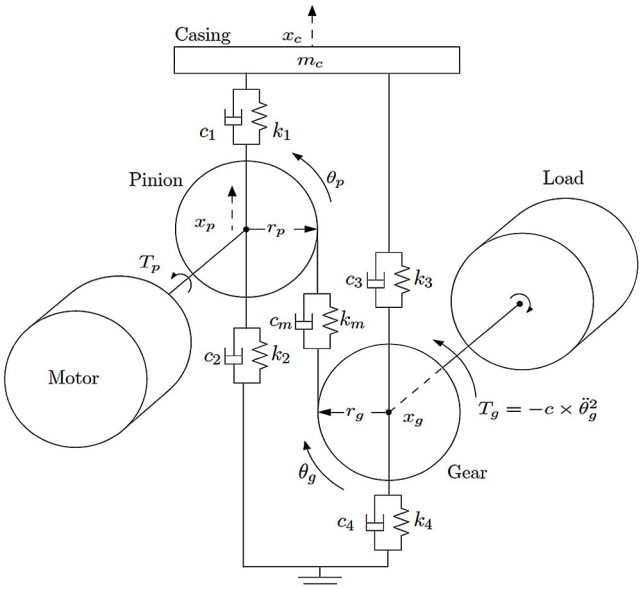

Figure 2. Gear model diagram

Hooke's Law by being linear in x. Standard viscous damping is assumed for all of the damping elements, with values that ensure that the system is highly underdamped. The gear is driven by the pinion, which in turn is subject to the pinion input torque T_p. The load on the gear is proportional to the second power of the gearwheel speed $T_g = K_s\dot{\theta}_2^2$ through the proportionality constant K_s. This allows the system to accelerate until equilibrium is reached. The proportionality constant K_s is selected at 0.4, so that the pinion rotates at about 240 r/min under an applied load of 500 Nm.

In this paper, a single gear fault is simulated by reducing the tooth mesh stiffness by 6% for the duration that the individual tooth that is affected is in mesh.

The differential equations are rewritten in state space notation and solved using Matlab's ode45 solver. The reader is referred to[14] for the written-out differential equations and parameter values. White noise is added to the signal so as to obtain a signal-to-noise ratio of 25 dB.

3.2 *Operating conditions*

Two loading conditions are investigated, namely a steady-state operating condition (constant torque) and also a loading condition where the applied torque varies with time. The time-varying load is chosen as arbitrary, and simply aims to illustrate the effect on the signal of both applying a slow and a slightly faster time-varying torque component. Since the speed is proportional to the applied torque, the time-varying torque induces amplitude, frequency and phase modulation. The operating conditions are summarised in Table 1.

Table 1. Instantaneous applied torque

	Applied load
Steady-state operations	$T_d(t) = 500$
Fluctuating operations	$T_d(t) = 500 \times [1+0.1\sin(2\pi t)+0.03\sin(6\pi t)]$

The time domain vibration responses as simulated on the gearbox casing for fluctuating operating conditions are indicated in Figures 3(a) and (b). Amplitude modulation is clearly observed, and under closer zoom significant frequency modulation is also seen.

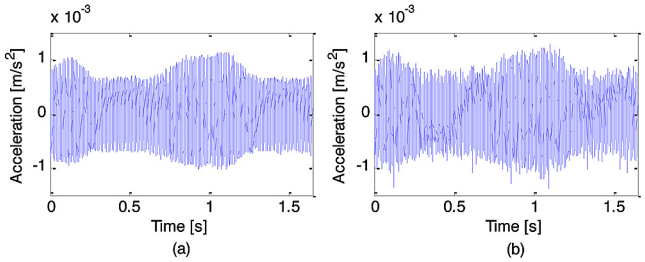

Figure 3. (a) Time domain waveform of the healthy gearbox (fluctuating operating conditions); (b) time domain waveform of gear casing response for one damaged tooth (fluctuating operating conditions)

The power spectral densities (PSDs) of the gear casing vibration simulated under steady-state operating conditions and fluctuating operating conditions, respectively, are illustrated in Figures 4(a) and (b). The dotted red lines correspond to the gear meshing frequency (GMF) components at approximately 90 Hz. The GMFs, along with their higher harmonics, dominate the vibration signal.

Figure 4(b) also indicates how the higher-order harmonics are increasingly prone to spectral smearing due to the frequency modulation.

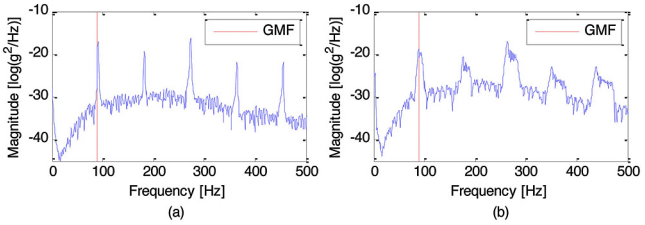

Figure 4. (a) PSD of gear casing response (steady-state operations); (b) PSD of the gear casing (fluctuating operating conditions)

4. Implementation and results

4.1 *Residual signals*

Both the AR and the NN filters were implemented using 20 time series datum points (*ie* $p = 20$). Separate models were trained for the stationary and the time-varying operating conditions. The abundance of training data (healthy data are readily available) simplifies the requirement to perform cross-validation.

The results for the stationary operating conditions are not illustrated, but both the AR and the NN residual signals clearly indicate the presence of the fault-induced signal deviations.

The highly non-linear signals, as simulated for the fluctuating operating conditions, are investigated next. Figures 5(a) and (b) illustrate the residuals computed for the damaged gearbox using the AR and NN filters, respectively. The AR model completely fails to detect the fault-induced outliers, while the NN successfully detects them. Figures 5(c) and (d) illustrate the envelopes as computed for the obtained AR and NN residuals, respectively.

It should be noted that the amplitudes of the impulses indicated in Figure 5 are fairly consistent. In some scenarios, it

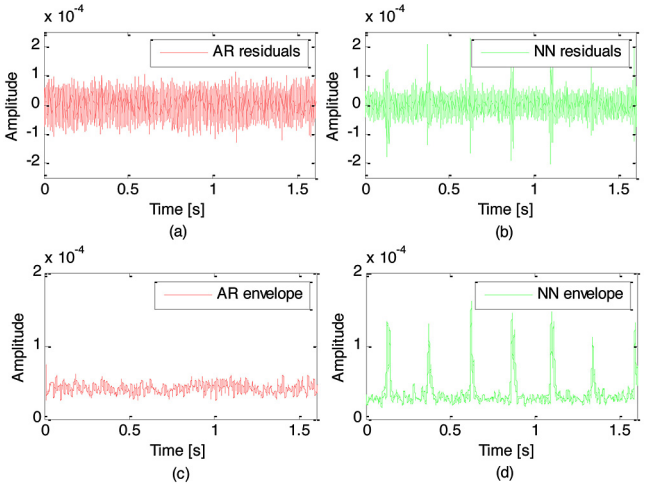

Figure 5. (a) AR residuals for damaged gearbox (fluctuating operating conditions); (b) NN residuals for damaged gearbox (fluctuating operating conditions); (c) envelope of AR residuals; (d) envelope of NN residuals

may be expected that the fault-induced amplitudes may be more stochastic due to the physical mechanism of the damage, or be more load dependent. In those cases, both envelope spectrum and cepstrum will be prone to greater inaccuracies.

4.2 *Sensorless relative speed estimation*

The relative speed is subsequently estimated based on the spectrogram of the vibration signal.

Figure 6(a) illustrates a contour plot of the local maxima as estimated from the spectrogram of the vibration signal, where the damaged gearbox was simulated under fluctuating operating conditions.

Figure 6(b) indicates the local maxima, which were clustered together based on the distances (modulus of the time, frequency and amplitude differences) between neighbouring points. Beginning at a manually selected point (0 s, 280 Hz), the clustering algorithm is used to group together all the local maxima, which are related to the third GMF harmonic.

Figure 6(c) plots both the true values (continuous blue line), which correspond to the third GMF harmonic (computed based on the true shaft angular velocity), as well as the values estimated based on the spectrogram (dashed red line). The estimated values are obtained by low-pass filtering the clustered local maxima. The estimated shaft angular speed corresponds fairly well to the global trends of the true angular speed, however, it fails to detect the rapid speed fluctuations (shaft jitter).

Figure 6(d) illustrates the contour plot of the local maxima for the resampled vibration signal. The low-frequency components are now fairly well corrected for, however, some of the higher-order frequency components (for example at approximately 360 Hz and 450 Hz) are still significantly smeared.

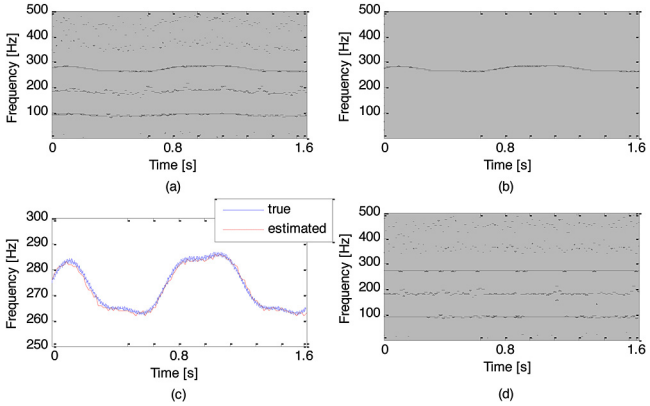

Figure 6. (a) Contour plot of the local spectrogram maxima; (b) the clustered local maxima, which corresponds to the third harmonic of the GMF; (c) the estimated and true instantaneous values of the third harmonic of the GMF; (d) contour plot of the local spectrogram maxima of the resampled vibration signal

Figures 7(a) and (b) illustrate the log PSDs of the original vibration waveform and the PSD of the resampled vibration waveform, respectively. When these spectra are compared to the undamaged PSDs, very little or no difference could be discerned in the amplitude of the gear meshing component (91 Hz or 22nd pinion shaft order). A log scale is used in this Figure to illustrate that no significant sidebands can be detected around the GMF, at

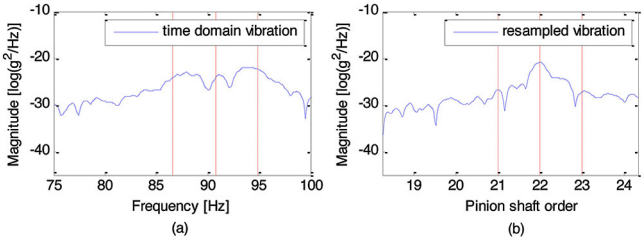

Figure 7. PSDs for the damaged gearbox (fluctuating operations) computed based on (a) the time domain vibration waveform and (b) the resampled vibration waveform. The continuous red line indicates the meshing frequency while the dashed red lines correspond to the expected sidebands, which correspond to the pinion shaft rotational frequency

intervals which correspond to the pinion shaft frequency.

Figures 8(a) and (b) illustrate the PSDs of the original discrepancy signal and the PSD of the resampled discrepancy signal of the damaged pinion, respectively. A clear difference in magnitude at the first pinion shaft order (4.1 Hz) component is observed when these PSDs are compared to their counterparts for the undamaged gearbox.

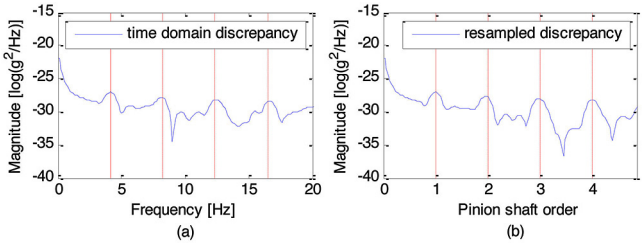

Figure 8. PSDs for the damaged gearbox (fluctuating operations) for (a) the discrepancy signal and (b) the resampled discrepancy signal

The discrepancy signal is impulsive in nature and thus not well suited to frequency analysis, which assumes sinusoidal base functions. Spectral analysis of an impulsive waveform tends to give rise to a spectrum that exhibits multiple harmonics, which are spaced at regular intervals. These intervals correspond to the periodicity of the impulses. Cepstrum analysis is efficient in collecting those families of harmonics and representing them in a concise manner.

Figure 9(a) represents the real cepstrum of the NN discrepancy signal, where the damaged gearbox was subjected to fluctuating operating conditions. Energy is observed at approximately 0.24 s, which corresponds with the rotational period of the pinion. Figure 9(b) represents the real cepstrum of the resampled NN discrepancy signal. The unit of the transform

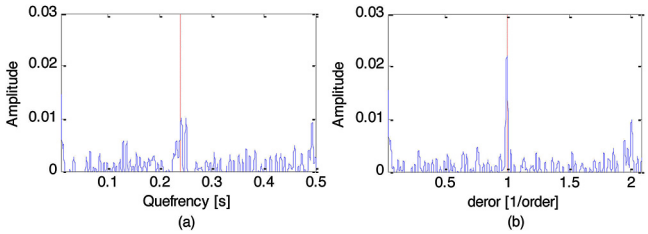

Figure 9. (a) Cepstrum of the NN discrepancy signal (fluctuating operations); (b) cepstrum of the resampled NN discrepancy signal (referred to as deror)

is referred to as derors (based on the cepstrum convention of frequency-quefrency and order-deror). Significant energy is clearly observed at 1 deror, which corresponds with the rotational period of the pinion.

As an interesting side note, it might be mentioned that smaller levels of pinion tooth damage generally tend to be more visible in the PSD of the resampled discrepancy signal than in its cepstrum. For this reason, it is advised that both the spectra and the cepstra of resampled discrepancy signals should be monitored.

5. Conclusion

This paper proposes that discrepancy (envelope residual) analysis and approximate signal resampling may jointly be used to monitor the condition of rotating machines that are subject to fluctuating operations and where an accurate measurement of the shaft angular position is not available. The proposed methodology firstly employs a neural network to remove the regular components from the time-varying vibration waveform. The envelope of the residual signal is subsequently computed so as to obtain a discrepancy signal. It is argued that the discrepancy signal is generally more informative and is also simpler (smoother) than the original waveform. This renders the discrepancy signal less sensitive to noise in the shaft angular velocity reference signal. It subsequently becomes more viable to use a shaft speed reference speed that has been directly estimated from the vibration signal to resample the discrepancy signal.

The methodology was investigated on data from a simple gear model, where a single tooth was damaged and where the gearbox was subject to a time-varying torque and angular speed. The results appear encouraging and future work should be conducted that investigates the proposed methodology on a range of real vibration datasets.

References

1. A K S Jardine, D Lin and D Banjevic, 'A review of machinery diagnostics and prognostics implementing condition-based maintenance', Mechanical Systems and Signal Processing, Vol 20, No 7, pp 1483-1510, 2006.
2. C J Stander and P S Heyns, 'Instantaneous angular speed monitoring of gearboxes under non-cyclic stationary load conditions', Mechanical Systems and Signal Processing, Vol 30, No 4, pp 817-835, 2005.
3. F Bonnardot, M El Badaoui, R B Randall, J Danière and F Guillet, 'Use of the acceleration signal of a gearbox in order to perform angular resampling (with limited speed fluctuation)', Mechanical Systems and Signal Processing, Vol 19, pp 766-785, 2005.
4. J Urbanek, T Barszcz, N Sawalhi and R B Randall, 'Comparison of amplitude-based and phase-based methods for speed tracking in application to wind turbines', Metrology and measurement systems, Vol 18, No 2, pp 295-304, 2011.
5. F Combet and L Gelman, 'An automated methodology for performing time synchronous averaging of a gearbox signal without speed sensor', Mechanical Systems and Signal Processing, Vol 21, pp 2590-2606, 2007.
6. F Combet and R Zimroz, 'A new method for the estimation of the instantaneous speed relative fluctuation in a vibration signal based on the short timescale transform', Mechanical Systems and Signal Processing, Vol 23, No 4, pp 1382-1390, 2009.
7. F Millioz and N Martin, 'Time-frequency segmentation for engine speed monitoring', special session on Pattern Recognition in Acoustics and Vibration, Proceedings of the Thirteenth International Congress on Sound and Vibration, ICSV13, Vienna, Austria, 2-6 July 2006.
8. R Zimroz, F Millioz and N Martin, 'A procedure of vibration analysis from planetary gearbox under non-stationary cyclic operations for instantaneous frequency estimation in time-frequency domain', Proceedings of Condition Monitoring, Stratford-upon-Avon, UK, 2010.
9. R Zimroz, T Barszcz, J Urbanek, W Bartelmus, F Millioz and N Martin, 'Measurement of instantaneous shaft speed by advanced vibration signal processing – application to wind turbine gearbox', Metrology and Measurement Systems, Vol XVIII, No 4, pp 701-712, 2011.
10. K Gryllias and I Antoniadis, 'Application of the energy operator separation algorithm (EOSA) for the instantaneous amplitude and frequency calculation of non-linear dynamic systems response', Proceedings of the ASME International Design Engineering Conference and Computers and Information in Engineering Conference IDECT/CIE, San Diego, USA, 2009.
11. Y Christos, K Gryllias and I Antoniadis, 'Instantaneous frequency in rotating machinery using a harmonic signal decomposition (HARD) parametric method', Proceedings of the ASME International Design Engineering Conference and Computers and Information in Engineering Conference IDECT/CIE, San Diego, USA, 2009.
12. R M Stewart, 'Some useful data analysis techniques for gearbox diagnostics', Proceedings of Meeting on Applications of Time Series Analysis, ISVR, Southampton, UK, pp 18.1-18.19, 1977.
13. W Wang and A K Wong, 'Autoregressive model-based gear fault diagnosis', Journal of Vibration and Acoustics, Transactions of the ASME, Vol 124, No 2, pp 172-179, 2002.
14. T Heyns, S J Godsill, J P de Villiers and P S Heyns, 'Statistical gear health analysis which is robust to fluctuating loads and operating speeds', Mechanical Systems and Signal Processing, Vol 27, pp 651-666, 2011.
15. J Antoni and R B Randall, 'Differential diagnosis of gear and bearing faults', Journal of Vibration and Acoustics, Transactions of the ASME, Vol 124, No 2, pp 165-17, 2002.
16. R Zimroz and W Bartelmus, 'Application of adaptive filtering for weak impulsive signal recovery for bearings local damage detection in complex mining mechanical systems working under condition of varying load', Solid State Phenomena, 180, pp 250-257, 2012. doi:10.4028/www.scientific.net/SSP.180.250
17. R Makowski and R Zimroz, 'Adaptive bearings vibration modelling for diagnosis', Lecture Notes in Comp Sci (in Lecture Notes in Artificial Intellig), LNAI, 6943, pp 248-259, 2011.
18. S J Godsill and P J W Rayner, Digital Audio Restoration – A

Statistical Model-Based Approach, Springer-Verlag, London, 1998.
19. C M Bishop, Pattern Recognition and Machine Learning, Springer, New York, 2006.
20. W Bartelmus, 'Mathematical modelling and computer simulations as an aid to gearbox diagnostics', Mechanical Systems and Signal Processing, Vol 15, No 5, pp 855-871, 2001.
21. W Bartelmus, F Chaari, R Zimroz and M Haddar, 'Modelling of gearbox dynamics under time-varying non-stationary operation for distributed fault detection and diagnosis,' European Journal of Mechanics – A/Solids, 29, pp 637-646, 2010.
22. M T Khabou, N Bouchaala, F Chaari, T Fakhfakh and M Haddar, 'Study of a spur gear dynamic behaviour in transient regime', Mechanical Systems and Signal Processing, Vol 25, No 8, pp 3089-3101, 2011.
23. S Jia, I Howard and J Wang, 'The dynamic modelling of multiple pairs of spur gears in mesh including friction and geometrical errors', International Journal of Rotating Machinery, Vol 9, No 6, pp 437-442, 2003.